

Power Load Dependencies of Cold Electron Bolometer Optical Response at 350 GHz

Mikhail A. Tarasov, Valerian S. Edelman, Andrey B. Ermakov, Sumedh Mahashabde, and Leonid S. Kuzmin

Abstract— Cold electron bolometers integrated with twin-slot antennas have been designed and fabricated. Optical response was measured in 0.06-0.6 K temperature range using black body radiation source at temperature 2-15 K. The responsivity of $0.3 \cdot 10^9$ V/W was measured at 2.7 K radiation temperature. The estimated ultimate dark responsivity at 100 mK can approach $S_v = 10^{10}$ V/W and reduces down to $1.1 \cdot 10^8$ V/W at 300 mK for the sample with absorber volume of $5 \cdot 10^{-20}$ m³. At high power load levels and low temperatures the changes of tunneling current, dynamic resistance and voltage response have been explained by non-thermal energy distribution of excited electrons. Distribution of excited electrons in such system is of none-Fermi type, electrons with energies of the order of 1 K tunnel from normal metal absorber to superconductor instead of relaxing down to thermal energy kT_c . This effect can reduce quantum efficiency of bolometer from hf/kT_{ph} in ideal case down to single electron per signal quantum in the high power case.

Index Terms—bolometers, nanofabrication, slot antennas, submillimeter wave technology, superconducting devices

I. INTRODUCTION

Cold-electron bolometer with Superconductor-Insulator-Normal metal-Insulator-Superconductor (SINIS) structure has promising predicted performance [1,2]. Under microwave irradiation additional excited electrons with high excess energy provide increase in tunneling current and/or decrease of dc voltage and such response is dependent on applied power and frequency. Usually for theoretical estimations it is assumed that microwave radiation is equivalent to dc heating at the same absorbed power. In such process the electron temperature of absorber is increased over the phonon temperature.

However in normal metal for Terahertz radiation at frequency $f \gg kT/h$ dominates quantum absorption of photons with energy $E = hf \gg kT$ by single electrons [3-6]. In this case the energy distribution of electrons is determined by a balance of processes of photon quantum absorption, electron-electron, electron-phonon, phonon-electron, phonon escape processes, and tunneling of excited electrons in a SIN junction [3,4]. This distribution function is significantly different from

equilibrium Fermi distribution. Microscopic calculations of tunneling current in clean limit [3,4] for electron-electron and electron-phonon collision integrals show that increase of response is dependent on multiplication of excited electrons with energies $\epsilon > kT$ due to electron-electron interactions and reabsorption of nonequilibrium phonons that did not escape from absorber. Multiplication of non-equilibrium electrons leads to increase of current response $\delta I(P)$, in which P – absorbed power, and this multiplication leads to increase in current δI for voltage bias mode. Thus current response δI of SINIS detector can exceed the photon counter limit of e/hf , but still being below the bolometric response limit of e/kT . Studies and optimization of energy relaxation in electron system at low temperatures can help to improve the practical optical response of SINIS detectors.

In our earlier experiments [7,8] we observed voltage response $\delta V(I) = V_{I,P=0} - V_{I,P}$, which shows that there is no thermal equilibrium in electron system. Now we performed detail analysis of new experimental data on IV curves, dynamic resistance, optical response to show absence of equilibrium in electron system and significant tunnel current due to electrons with excess energy.

II. EXPERIMENT

Bolometers containing 3 serial SINIS structures were integrated in twin-slot antennas. Bottom layer of bolometer was made of normal-metal Al absorber 10 nm thick in which superconductivity was suppressed by underlayer of ferromagnetic film [9]. For microwave signal such bolometers were connected in parallel by means of capacitive connection. Dimensions of elements: area of tunnel junctions $0.25 \mu\text{m}^2$, length, width and thickness of normal metal strip between tunnel junctions $1 \cdot 0.1 \cdot 0.01 \mu\text{m}^3$, dc resistance of single absorber $\sim 200 \Omega$. Parallel connection for microwave signal makes antenna load of 60Ω . Tunnel junctions parameters were similar to earlier studied in [7,8]. When cooling down to $T < 0.1$ K the resistance ratio $R_d(V=0)/R_n$ (in which $R_d = dV/dI$, R_n - asymptotic normal resistance) approached $R_d/R_n = 15000$, and total resistance of array at 0.1 K approached $R_{d(V=0)} = 400 \text{ M}\Omega$.

Samples were measured in dilution cryostat equipped with pulse tube refrigerator [10]. Additional recondensing stage with liquefying of He gas in a 0.12 liter container allows to keep temperature below 0.1 K during 4-5 hours with compressor shut down. Chip with SINIS receiver was mounted inside copper radiation shield at temperature 0.4-0.45 K, in which inner wall was painted with black absorber containing Stycast® 2850FT.

Manuscript received on May 29, 2014. This work was supported in part by the Swedish Space Agency SNSB and Swedish scientific agency Vetenskaps Rådet.

M.A.Tarasov and A.B.Ermakov are with the V.Kotelnikov Institute of Radio Engineering and Electronics of Russian Academy of Sciences, 125009 Moscow, Russia (phone: 7-495-6293418; fax: 7-495-6293678; e-mail: tarasov@hitech.cplire.ru).

V.S.Edelman is with the P.Kapitza Institute for Physical Problems of Russian Academy of Sciences, Moscow, Russia.

S.Mahashabde and L.S.Kuzmin are with the Chalmers University of Technology, Gothenburg, Sweden.

Silicon chip 0.35 mm thick was attached to sapphire hyperhemisphere 10 mm in diameter that collect radiation to the planar antenna. Lens itself was glued with Stycast® 1266 in copper holder screwed to the dilution chamber. Measurements with RuO₂ thermometer glued to Si plate instead of detector show that its temperature at 0.1 K differs by less than 2-3 mK from mixing chamber temperature measured by LakeShore® thermometer with absolute error below 5 mK.

In front of lens in the bottom of radiation shield it was a hole 5 mm in diameter, which was covered with planar bandpass filters [11] for central frequency of 330 GHz and total passband of 50 GHz. Spectral transmission within 10% accuracy is described by product of two Lorentz lines with halfwidth of 70 GHz. Transmission in the maximum was over 90%. Distance from lens to filter is 2-3 mm, between filters 2 mm, from filter to black body source 2-3 mm.

Radiation source is a black body made of Si wafer covered with NiCr film of square resistance of 300 Ω. Wafer was mounted on heat insulating legs to 1 K pot. Temperature of radiation source was monitored by resistance of a calibrated RuO₂ chip-resistor and heating varied by current through this NiCr film in the range of 0.9-15 K. Dissipated power was up to few milliwatts, time constant for heating/cooling of the order of 0.1 s.

Power received by antenna was calculated using Planck formula for single mode

$$P_{\text{incident}} = \int df \frac{hf}{\exp\left(\frac{hf}{kT_R}\right) - 1} * K1 * K2 * K3 \quad (1)$$

in which T_R - radiation source temperature, factors $K1$ and $K2$ accounted for transmission of filters and spectral matching of antenna. For twin-slot antenna we take Lorentz line with half-width of 100 GHz and maximum at 330 GHz. Influence of $K2$ was rather small, below 20%. Multiplier $K3=0.72$ takes into account reflection of sapphire-silicon and sapphire-vacuum interfaces.

III. EXPERIMENTAL IV CURVES AND ESTIMATIONS OF ELECTRON TEMPERATURE

Equivalent electron temperature in normal metal absorber was deduced from dependencies of dynamic resistance $R_d=dV/dI$ and comparison with dV/dT dependence of ideal SIN junction at some effective electron temperature. In Fig. 1a,b presented IV curves for two electron temperatures and calculation according to simple analytic relation (2). IV curve of ideal SIN junction for voltages below the gap of superconductor $V_\Delta=\Delta/e$ (in which Δ — energy gap of superconductor), for single junction can be presented as [12]:

$$I(V,T) = \frac{1}{eR_n} \sqrt{2k\pi T_e e V_\Delta} \exp\left(-\frac{eV_\Delta}{kT_e}\right) \sinh\left(\frac{eV}{kT_e}\right) \quad (2)$$

In our case we have 6 junctions connected in series, so measured values of R_n and V are divided by 6 to fit with model curve. Voltage derivative of current brings dynamic conductivity and inverse value is dynamic resistance. In

experimental curves measured voltage corresponds to $6V_{\text{sin}}$ in which V_{SIN} — voltage across the single SIN junction.

Gap voltage V_Δ in (2) according to BCS theory corresponds to $eV_\Delta=\Delta(0)=1.76*kT_c$ in which T_c — critical temperature. It can be determined from the dependence $R_d(T, V=0)$, which in the temperature range $\sim 0.3 - 0.5$ K has exponential shape. At higher temperatures it should be accounted also the temperature dependence $\Delta(T)$, and at temperatures below 0.2 K dynamic resistance R_d approaches constant value that is explained by overheating of electron system by external radiation. Value of equivalent T_e can be estimated by fitting with equation (2). In our case using $\Delta=k*2.45$ K we obtained good correspondence of experimental calculated curves in all figures. Small difference can be observed at $V>0.4-0.5$ mV, where resistance is higher compared to calculated one due to electron cooling. In our fitting we use value of Δ that corresponds to $T_c\sim 1.4$ K. In measurements at $T=1.5$ K IV curve is linear and at 1.3 K nonlinearity is clear visible, so T_c is within this range.

If electron system is excited by radiation, then dependence is different from heating of sample, see fig. 1b. There is no more correspondence with simple thermal model. If we take T_e for which $R_d(V=0)$ is the same as in model, then at higher bias current the difference in resistance can be more than 10 times larger. One can see that power response and temperature response are different at 70 mK and coincide at 340 mK (Fig. 2).

Dependencies of responsivity $d\delta V/dP$ on phonon temperature and equivalent electron temperature are presented in Fig. 3a,b for radiation power levels 0.22 pW, 1.35 pW, 2.95 pW, 4.95 pW. When plotted in dependence on electron temperature (b) the shape of dependence is more natural and shows that responsivity is dependent on nonequilibrium electron temperature. When irradiated at 5 pW load the responsivity is reduced by an order of magnitude compared to 0.2 pW power load. When bath is heated to 0.34 K these responsivities become equal for all power loads which means that in this range detector becomes linear, $d\delta V/dP$ is independent on power and is determined by temperature. In this case electron and phonon temperatures are very close, and nearly equal. It means that increase in bath temperature leads to increase of relaxation processes and thermalization of electron system.

Losses in bolometer can be roughly estimated from power to current transfer ratio, or current responsivity. Compare a number of incoming quanta $I_0=5*10^8$ s⁻¹ for 0.1 pW at frequency 330 GHz and number of excited electrons that tunnel due to irradiation $I_S=6*10^8$ s⁻¹ (current increase at this power load). Quantum efficiency $\eta=I_S/I_0=1.2$ is close to unity, which means that one quantum produce just one electron, that is a photon counter mode. There is no multiplication of excited electrons number which was predicted in [4] for bolometric mode of operation. If energy did not escape from electron system, then the number of excited electrons with energies in the range $\sim (0.2 - 1)\Delta$ should be 30 times more.

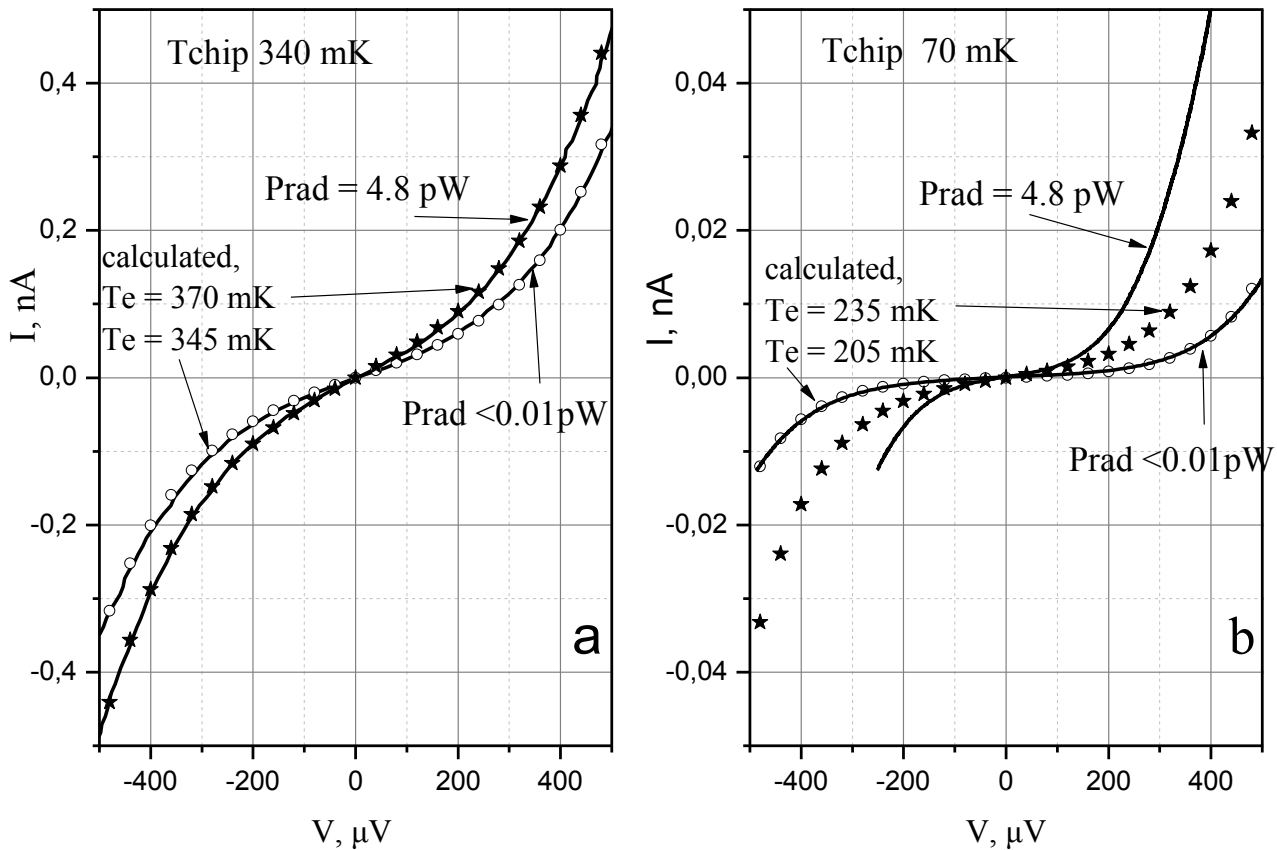


Fig. 1. IV curves of SINIS bolometer at bath temperature 340 mK (a) and 70 mK (b). Solid lines correspond to experimental data obtained at two radiation power levels of 4.8 pW and below 10 fW. Stars and circles – calculated curves for 370 mK and 345 mK (a), and 235 mK and 205 mK (b).

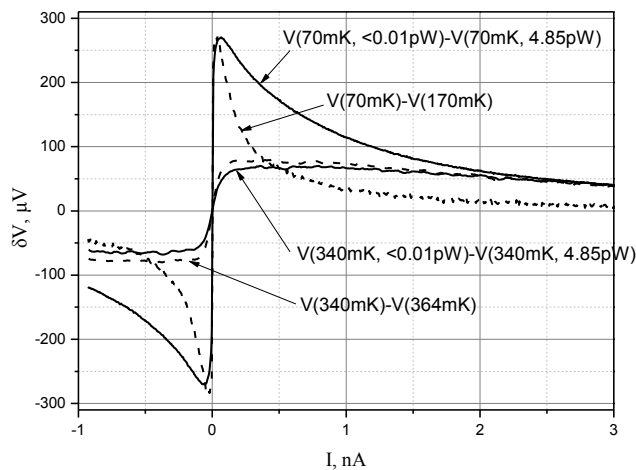


Fig. 2. Voltage response dependencies on dc bias for temperatures 70 mK and 340 mK. Solid lines under 4.85 pW irradiation, dashed- response to equivalent increase in temperature without irradiation.

IV. DISCUSSION

According to estimations [17] the difference of calculated and experimental curves proves the absence of equilibrium in electron system when energy distribution for electrons with energy above the Fermi energy and holes with energy below it does not correspond to Fermi distribution with equivalent electron temperature. These excited electrons can be viewed in two groups: thermalized and athermal. Impact of thermalized electrons can be estimated assuming that their temperature corresponds to calculated for the case when calculated curve tangential experimental at $V=0$, and dynamic resistance of both are equal. In Fig.1b such assumption leads to the electron temperature under irradiation estimation of 235 mK. The impact from athermal electrons can be estimated as a difference between measured and calculated and can be up to 70% of the total response. When temperature increase the relaxation processes speed-up and at 0.34 K the impact from athermal electrons is much less. At the same time impact from thermalized electrons increase, they prevail in tunneling current. As a result the voltage dependence of response approaching the calculated one.

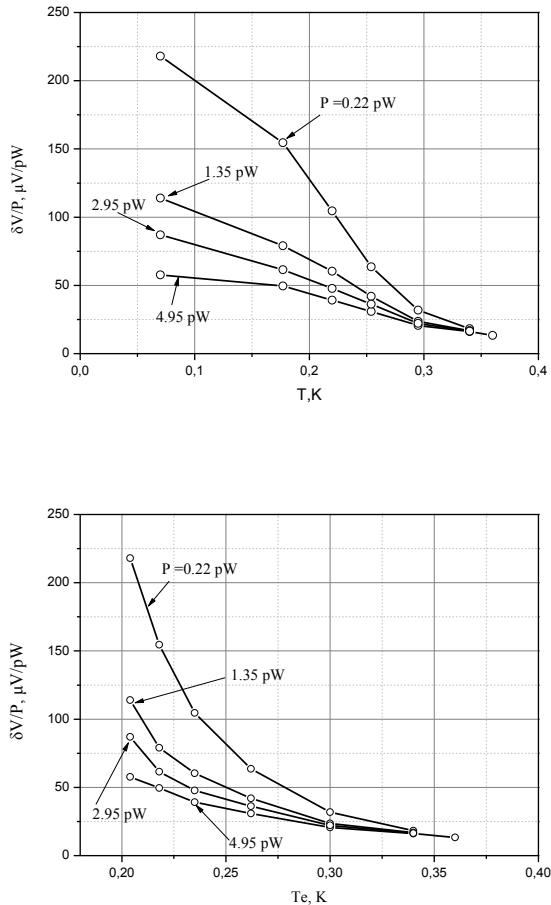


Fig. 3. Responsivity dependence on bath temperature (top panel) and on equivalent electron temperature (lower panel) for radiation power levels 0.22 pW, 1.35 pW, 2.95 pW, 4.95 pW.

Radiation power is collected in a normal metal absorber with dimensions much less compared to the wavelength, so it can be considered as a lumped element. When absorbing the radiation quantum energy $hf/k = 16$ K, all this energy is transferred to electron, it forms electron-hole pair with energies from 0 to hf above/below the Fermi energy. The average energy of excited electron and hole is 8 K.

Excited electrons and holes diffuse towards the area of tunnel junctions with diffusion time τ_{diff} , after that transfer into superconducting electrode with time constant τ_{sin} . During this period energy is redistributed due to electron-phonon, phonon-electron, electron-electron, phonon-phonon and phonon escape processes. As a result energy of excited electrons is reduced, their number can increase, some power escape into substrate and superconducting electrodes. Additional tunneling current under irradiation depends on ratio of time constants of these processes. Since all time constants are strongly dependent on excitation energy, the dynamics become very complicated, especially taking into account transition from two-dimensional to three dimensional cases when changing temperature and power. Processes in superconducting electrode will be also ignored; we assume it as a thermal sink.

Microscopic model described in [13] assume that as the result of electron-electron interaction primary electron after each inelastic collision will produce three new quasiparticles: two electrons and one hole. Each of them has $hf/6$ of initial energy. Absorption of one phonon will produce two quasiparticles: one electron and one hole, similar to photon absorption. Spontaneous emission of phonons preserves the number of quasiparticles. Rate of electron-electron collisions that are necessary for multiplication of electrons is an order of magnitude slower compared to electron-phonon relaxation which reduce excitation energy and do not lead to multiplication of quasiparticles. The phonon-electron process can slightly increase bolometer response above the photon counter limit.

Model of thermalization in normal metal is also discussed in [16]. According to this model the most probable process for energy relaxation of electron from energy level of $E=\Delta$ is down to $\Delta/4$ and emerging of phonon with energy $3\Delta/4$. This energy is much higher compared to thermal phonons and we obtain a nonthermal distribution for both phonons and electrons.

First we estimate the diffusion constant for electrons in normal metal:

$$D = \frac{1}{e^2 N \rho} \quad (3)$$

in which $\rho=0.07 \Omega \cdot \mu\text{m}$, $N=2.3 \cdot 10^{10} \mu\text{m}^{-3} \text{eV}^{-1}$ is electron density at Fermi level, this brings $D=0.004 \text{m}^2/\text{s}$. Diffusion time for electrons to travel the distance about $1 \mu\text{m}$ from the middle of absorber to tunnel junction area is $\tau_{diff}=0.25 \text{ns}$.

Relation of diffusion constant with speed v mean free path l is $D=lv/3$. Taking Fermi velocity $v_F=2 \cdot 10^6 \text{m/s}$ one can get the mean free path in absorber $l=6 \text{nm}$. Thickness of absorber in our samples is 10nm , which is comparable to mean free path. Diffusion time through the thickness of absorber is 0.025ps .

One more important parameter is a characteristic time for tunneling in SIN junction. Time constant for electrons to escape from normal metal to superconducting electrode is determined by time of many attempts providing close to unity probability to tunnel through the barrier. Transparency of barrier is related to normal resistance of junction. According to [3, 12], if in the bias point differential resistance is close to normal resistance, then tunneling time constant is

$$\tau_{sin} = N(0) e^2 R_n S t \quad (4)$$

in which N is density of states at Fermi level, R_n is normal resistance of junction, S junction area, t film thickness. For aluminum film 10nm thick, $R_n S \sim 1000 \Omega \cdot \mu\text{m}^2$, this corresponds to $\tau_{sin} \sim 40 \text{ns}$. As a result $\tau_{sin} \gg \tau_{diff}$ and distribution of electrons along the normal metal is uniform.

Nonequilibrium condition of system is mainly determined by relation between electron-electron and electron-phonon time constants. The last can be estimated similar to [13, 14] as:

$$\tau_{ep} = \frac{3 I_0 k^6 N(0)}{\Sigma E^4} \quad (5)$$

Parameter $I_0=25$, electron-phonon constant $\Sigma=2.3 \text{ nW}/(\mu\text{m}^3 \cdot \text{K}^6)$. For average excitation energy of electrons $E/k=8 \text{ K}$ it corresponds to $\tau_{ep}=0.2 \text{ ns}$, that is comparable to diffusion time. The wavelength of such phonons with energy 8 K and sound speed in aluminum $\sim 5000 \text{ m/s}$ equals to $\lambda_{\text{phonon}} \sim 30 \text{ nm}$ and it is larger compared to film thickness. It means that such phonons propagate at small angles to the boundary between Al absorber and Si substrate and probability of their escape to substrate is rather small. The last stage of electron-phonon interaction producing quasi-Fermi distribution happens at phonon temperature 340 mK or 70 mK with corresponding electron temperatures 370 mK and 235 mK for which electron-phonon power flow in absorber is 280 fW and 28 fW . Actually electrons interact with phonons of the entire volume of Al absorber and Al superconducting electrodes that is 10 times as large, this makes corresponding power flow up to 3 pW and 0.3 pW .

Opposite process of phonon-electron interaction is rather fast, according to [9,14]:

$$\tau_{pe} = \frac{234 N_A n_d k^3}{6 \Sigma \Theta_D^3 E^2} \quad (6)$$

In which $N_A n_d$ – atomic density that is for aluminum $6 \cdot 10^{22} \text{ cm}^{-3}$, $\Theta_D=428 \text{ K}$ – Debye temperature. If we take the distribution of energy from electron with initial energy 8 K to electron and phonon with the ratio 1:3, this corresponds to $\tau_{pe}(6 \text{ K})=5 \text{ ps}$.

The dynamics is quite different for electrons in the region of tunnel junctions. For acoustic waves both normal and superconducting electrodes separated by barrier below 2 nm thick is the same material and phonons can escape from normal into superconductor metal in few picoseconds without returning energy to electrons in absorber. Such process is a loss channel for energy that irreversibly escapes to superconductor or substrate. Characteristic time for such escape through the thickness of absorber t_{abs} is $\tau_{\text{escape}}=t_{\text{abs}}/v_{\text{sound}}=2 \text{ ps}$.

Phonon relaxation time can be estimated in the case of scattering at boundaries by dividing the characteristic length of our sample about $l_{\text{abs}}=3 \mu\text{m}$ by sound speed

$$\tau_{pp}=l_{\text{abs}}/v_{\text{sound}}=600 \text{ ps}.$$

Redistribution of energy among electrons is governed mainly by electron-electron interaction. Equation for calculating of such time constant τ_{ee} for two-dimensional case corresponding to thin normal absorber taken from [12,14]:

$$\tau_{ee} = \frac{hE_F}{\pi^2 E^2 \ln\left(\frac{E_F}{E}\right)} \quad (7)$$

in which $E_F=11.6 \text{ eV}$ – is Fermi energy. At electron temperature of 8 K this time is $\tau_{ee}=1 \text{ ns}$, that exceeds $\tau_{ep}=0.2 \text{ ns}$ for the same electron energy. For three-dimensional case τ_{ee} is dozens times as much compared to two-dimensional. Value of τ_{ee} becomes equal to τ_{sin} for temperatures in the range $(1 \dots 1.3) \text{ K}$. Value of τ_{ep} becomes equal to τ_{sin} for electron temperatures $\sim 2 \text{ K}$.

From the above review it is clear that due to complicated combination of electron-electron, electron-phonon, phonon-electron interactions which vary with signal frequency and

power, the energy distribution of electrons is much different from simple Fermi distribution. Nonequilibrium of system is mainly determined by ratio of escape time for electrons due to tunneling τ_{sin} to electron-electron and electron-phonon time constant. Finally, we can pick out two groups of time constants, first is energy independent, it is diffusion time $\tau_{\text{dif}}=0.25 \text{ ns}$, tunneling time $\tau_{\text{sin}}=40 \text{ ns}$, phonon escape time $\tau_{\text{esc}}=2 \text{ ps}$, and phonon-phonon time $\tau_{pp}=0.6 \text{ ns}$. Energy dependent time constants are second order dependent $1/E^2$ electron-electron time τ_{ee} and τ_{pe} , and also a fourth order dependent $1/E^4$ electron-phonon constant τ_{ep} . Dependencies are presented in Fig. 4.

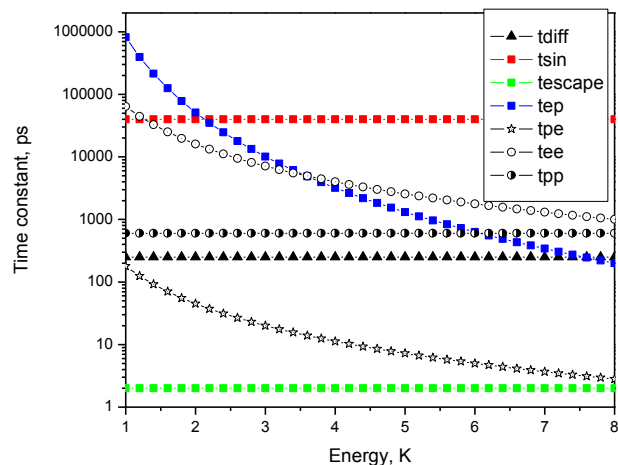


Fig. 4. Time constant dependencies on excitation energy plotted in Kelvins i.e. E/k.

Electron-electron and electron-phonon time constants become equal at energy around 3.7 K , and for lower energies electron-phonon interaction get slower, so electron-electron can become dominating. To increase bolometer efficiency the length of absorber should be increased providing diffusion time τ_{dif} longer compared to τ_{ee} and τ_{ep} , value of τ_{ep} should be increased by using absorber material with lower electron-phonon parameter σ ; resistivity, density, and acoustic impedance of absorber material should be increased as well. According to [3] the optimal resistance of SIN junction should be around $10 \text{ k}\Omega$.

V. VOLTAGE RESPONSE

In our experiments at low bias we observe significant maximum that is not presented in conventional model of SINIS bolometer without strong power load. This maximum is increasing with signal power level that contradicts to eventual explanation by Coulomb blockade that should increase with cooling and reducing of power level. In IV curves current increase is observed compared to the dark IV curve.

We assume that such additional maximum corresponds to direct detection at nonlinearity of SIN junction. At zero bias there is no detection because of IV symmetry for both half-periods of signal and for bias about $50\text{-}100 \mu\text{V}$ there is maximum of rectified signal at maximum of nonlinearity.

Contrary to bolometric detection here we have direct detection (rectification) of incoming signal. In Fig.5,6 presented response dependencies measured at black body source temperatures 0.89; 1.8; 2.25; 3.0; 3.6; 4.3; 4.9; 5.5; 6.0; 6.6; 7.2; 8.3; 9.8; 11.2; 12.5 K. Voltage response obtained by subtraction of adjacent IV curves.

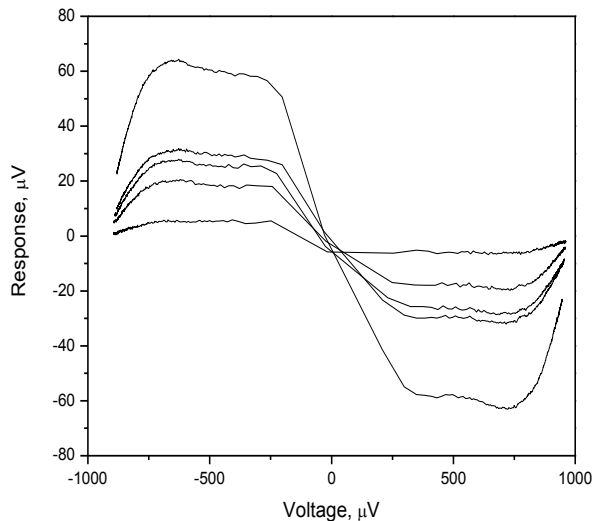


Fig. 5. Voltage response at lower levels of signal in the range 1-4 K. Standard bolometric response observed at about half-gap voltage bias, and at lower bias around quarter gap voltage corresponding to higher nonlinearity appears a direct detector response.

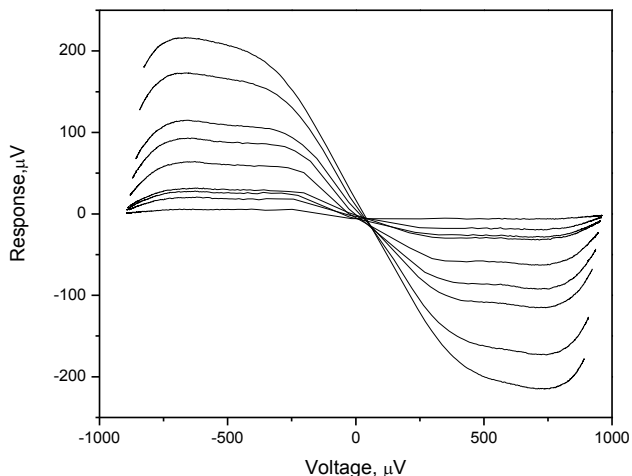


Fig. 6. Voltage response in wider radiation temperature range 1 - 15 K.

Simple calculation of second derivative of IV curve for SIN junction (Fig.7) shows that maximum curvature is presented at lower bias voltages. For comparison in Fig.8 similar dependencies is presented in logarithmic scale for three temperatures of sample. Curvature is increasing by four orders with cooling from 350 mK to 150 mK.

Nonlinearity of SIN junctions was earlier used for heterodyne and direct detection of microwave signals in [18,19], in which were used Pb/Bi/In-oxide-Ag junctions with area of $1.2 \mu\text{m}^2$ and specific capacitance of InOx of $4 \mu\text{F}/\text{cm}^2$.

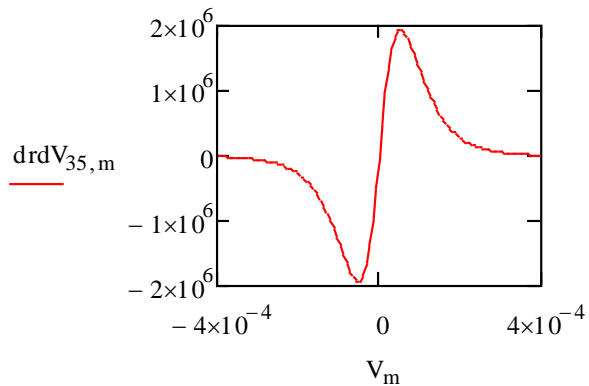


Fig. 7. Second derivative of normalized IV curve at 350 mK.

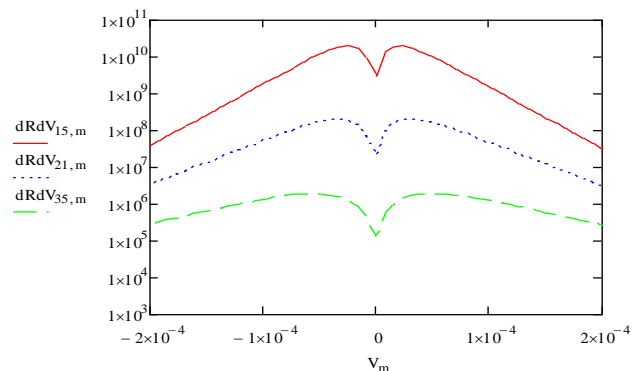


Fig. 8. Curvature dR/dV in logarithmic scale for temperatures 150, 210, 350 mK.

Noise temperature comparable to SIS junctions was demonstrated in such junctions when biased near the energy gap. Specific methods of fabrication for lead and niobium SIN junctions of $0.5 \mu\text{m}^2$ area are described in [20,21]. Noise temperatures down to 140 K were obtained at signal frequencies up to 320 GHz [22]. One more similar structure of SINS type is described in [23], for which the estimation of noise temperature is at the level of 13 K for signal frequency 330 GHz. Direct detectors in mm-wave band with $\text{NEP} = 10^{-15} \text{ W}/\text{Hz}^{1/2}$ [24] working at 4.2 K did not found practical applications, but for temperatures below 300 mK they can be competitive with superconducting bolometers. According to [25] the conventional current response at relatively low frequencies can be presented as

$$R_i^{cl} = \frac{d^2I/dV^2}{2*dI/dV} = \frac{S}{2} \quad (8)$$

In nonlinear SIN or SIS junction with responsivity $S/2 > e/hf$ this expression should be modified to the relation for quantum assisted tunneling

$$R_i^{QM} = \frac{e}{hf} \left[\frac{I(V+hf/e) - 2I(V) + I(V-hf/e)}{I(V+hf/e) - I(V-hf/e)} \right] \quad (9)$$

Assuming that shot noise is dominating in such detectors $i_n^2 = 2eIB$ we can estimate the NEP of matched detector as

$$\text{NEP} = \frac{\sqrt{2eIB}}{R_i^{QM}} \quad (10)$$

that can approach in quantum limit maximum value of $\text{NEP} = hf(2IB/e)^{1/2}$.

In our case at $T=100$ mK for bias current 0.01 nA and output band 1 Hz this corresponds to $2 \cdot 10^{-18}$ W/Hz^{1/2}, and comparable to estimations for bolometric response of SINIS structure. In this rough estimations we do not take into account input mismatch $\eta = \frac{4R_{rf}R_s}{(R_{rf}+R_s)^2}$, in which R_{rf} is antenna impedance and R_s is detector impedance. For planar antenna we can take source impedance of 70Ω . Active part of nonlinear detector impedance in quantum assisted tunneling limit is

$$R_{rf} = \frac{2hf/e}{I(V+hf/e)-I(V-hf/e)} \quad (11)$$

contrary to dynamic resistance in bias point for classical detector. This value will be partially shunted by SIN junction capacitance with specific value of about 60 fF/ μm^2 that is about 10Ω at signal frequency of 350 GHz.

For comparison we can also mention super-Schottky diodes with superconductor-semiconductor junctions Pb-GaAs that were first proposed in [26]. Shape of IV curve and detector response analytic theory for super-Schottky diodes were developed in [27]. Current response can be presented as

$$R_i = \frac{e}{2kT} \frac{\tanh(hf/2kT)}{hf/2kT} \quad (12)$$

This value approaches classical limit $R_{cl}=e/2kT$ for lower frequencies $hf \ll 2kT$ and quantum limit $R_q=e/hf$ for higher frequencies $hf > 2kT$. For $T=100$ mK the characteristic frequency separating two cases is only 5 GHz.

For our signal at 350 GHz the nonlinearity scale for quantum assisted tunneling corresponds to $dV \sim hf/e = 1.3$ mV, and energy gap of single Al SIN junction is only 0.2 mV. In this scale we cannot expect quantum detection, but low-frequency components of black body thermal radiation and external RF interferences like mobile telephones and TV stations will be detected and make impact to current as we can see in Fig. 6. Such detector effect can be assumed as significant for frequencies below 50 GHz for bias close to zero and for frequencies below 100 GHz for bias around the gap voltage.

VI. CONCLUSION

For SINIS detectors nonequilibrium in electron system plays the main role in optical response performance. Ultimate parameters can be achieved for maximum multiplication of electrons in absorber due to electron-electron interactions and absorption of nonequilibrium phonons. Time of electron-electron collisions is relatively big at the beginning of such process and diminish multiplication. Nonequilibrium of phonon system is determined by freedom of phonon escaping to superconducting electrode that is fabricated from the same aluminum as absorber. The natural way to increase multiplication and response of detector is using material with lower τ_{ee} , higher τ_{ep} , and higher acoustic mismatch with aluminum, that can be Hafnium. Inversion of sequence of layers with placing absorber above superconductor can also reduce phonon escape to substrate.

REFERENCES

1. L. Kuzmin, On the concept of a hot-electron microbolometer with capacitive coupling to the antenna, *Physica B: Condensed Matter*, **284-288**, 2129 (2000).
2. L. Kuzmin, Array of cold-electron bolometers with SIN tunnel junctions for cosmology experiments, *Journ. of Phys.s: Conf. Ser.* **97** (2008) 012310
3. I.Devyatov, M.Kupriyanov, Investigation of a nonequilibrium electron subsystem in low-temperature microwave detectors, *JETP Lett.*, v.**80**, No. 10, pp. 646-650 (2004).
4. I.Devyatov, P.Krutitsky, M.Kupriyanov, Investigation of various operation modes of a miniature superconducting detector of microwave radiation, *JETP Lett.*, v.**84**, No.2, pp.57-61 (2006).
5. A.Semenov, I.Devyatov, M.Kupriyanov, Theoretical analysis of the operation of the kinetic-inductance based superconducting microwave detector, *JETP Lett.*, v.**88**, No.7, pp.514-520 (2008).
6. P. Virtanen, T.T. Hekkila, F.S. Bergeret, and J.C. Cuevas, Theory of microwave-assisted supercurrent in diffusive SNS junctions, *Phys. Rev. Lett.* **104**, 247003 (2010).
7. M.Tarasov, L.Kuzmin, V.Edelman, et al., Optical response of a cold-electron bolometer array, *JETP Lett.*, v.**92**, No.6, p. 416-420 (2010).
8. M.Tarasov, V.Edelman, L.Kuzmin, P. de Bernardis, S.Mahashabde, Optical response of a cold-electron bolometer array integrated in a 345 GHz cross-slot antenna, *IEEE Trans. Appl. Supercond.*, vol.**21**, no. 6, pp. 3635 (2011)
9. M.A.Tarasov, L.S.Kuz'min, N.S.Kaurova, Thin multilayer aluminum structures for superconducting devices, *Instr. and Exp. Techn.*, Vol. 52, No. 6, pp. 877-881 (2009).
10. V.Edelman, G.Yakopov, A dilution microcryostat cooled by a refrigerator with an impulse tube, *Instr. and Exp. Techn.*, vol.56, № 5, pp. 613-615 (2013).
- 11 M.A. Tarasov, V.D. Gromov, G.D. Bogomolov, et al., Production and characteristics of grid band-pass filters, *Instr. and Exp. Techn.*, 2009, Vol. 52, No. 1, pp. 74–78 (2009).
12. G. O'Neil, Improving NIS tunnel junction refrigerators: modelling, materials, and traps, Ph.D. Thesis, Univ. Colorado, 2011.
13. J N Ullom, P A Fisher, Quasiparticle behavior in tunnel junction refrigerators, *Physica B*, vol. 284-288, pp. 2036–2038 (2000).
14. G. C. O'Neil, P. J. Lowell, J. M. Underwood, J. N. Ullom, Measurement and modeling of large area normal-metal/insulator/superconductor refrigerator with improved cooling, *Phys. Rev. B* 85, 134504 (2012)
15. D.Golubev, L.Kuzmin, Nonequilibrium theory of the hot-electron bolometer with NIS tunnel junction, *J.Appl. Phys.*, vol. 89, No 11, 6464-6472 (2001)
16. W.S. Holland, E.L. Chapin, A. Chrysostomou, et al., 2013, arXiv:1301.3650v1 [astro-ph.IM].
17. M.Tarasov, V.Edelman, S.Mahashabde, L.Kuzmin, Nonthermal optical response of tunnel structures superconductor-insulator-normal metal-insulator-superconductor, *JETPh*, vol. 118(145), № 6 (2014).
18. R.Blundell, K.H.Gundlach, A quasiparticle SIN mixer for the 230 GHz frequency range, *Int. J. Infrared and MM waves*, Vol. 8, No. 12, 1573-1579 (1987).
19. S.Rudner, M.J.Feldman, E.Kollberg, T.Claeson, Superconductor-insulator-superconductor mixer with arrays at millimeter-wave frequencies, *J.Appl. Phys.*, 52, 6372, 1981
20. T.Lehnert, K.H.Gundlach, Fabrication and properties of superconductor-insulator-normal metal tunnel junctions, *J.Vac. Sci. Technol.*, A 10(1), pp. 110-114 (1992).
21. D.Winkler, T.Claeson, High-frequency limits of superconducting tunnel junction mixers, *J.Appl.Phys.*, **62**, 4482 (1987)
22. D.Mailer, A.Karpov, T.Lehnert, K.H.Gundlach, Superconductor-insulator-normal conductor tunnel junctions for frequency mixing around 300 GHz, *J.Appl. Phys.*, 78 (3), pp. 2113-2116 (1995).
23. A.Karpov, D.Maier, J.Blondel, B.Lazareff, K.H.Gundlach, Noise and thermal properties of a submillimeter mixer with the SINIS tunnel junction, *Int. J. IR & MM Waves*, Vol. 16, No. 8, pp. 1299-1315 (1995).
24. H.J.Hartfuss, K.H.Gundlach, Video detection of mm-waves via photon-assisted tunneling between two superconductors, *Int. J. IR & MM Waves*, Vol. 2, No. 4, pp. 809-827 (1981).
25. P.L.Richards, T.-M.Shen, Superconductive devices for millimeter wave detection, mixing and amplification, *IEEE Trans. Electron. Dev.*, ED-27, No. 10, pp. 1909-1920 (1980).
26. M.Mccoll, M.F.Millea, A.H.Silver, The superconductor-semiconductor Schottky barrier diode detector, *Appl. Phys. Lett.*, Vol. 23, pp. 263-264 (1973).
27. J.R.Tucker, Quantum limited detection in tunnel junction mixers, *IEEE J. of Quantum Electronics*, QE-15, No. 11, pp. 1234-1258 (1979).